# Xylose-Based Polyethers and Polyesters *via* ADMET Polymerization toward Polyethylene-Like Materials

*Marco Piccini,*[†] *Jasmine Lightfoot,*[†] *Bernardo Castro Dominguez*[‡] *and Antoine Buchard**[,†]

[†] Centre for Sustainable and Circular Technologies, Department of Chemistry, University of Bath, Claverton Down, BA2 7AY, United Kingdom

[‡] Department of Chemical Engineering, University of Bath, Claverton Down, BA2 7AY, United Kingdom

KEYWORDS: renewable resources, bio-based polymers, carbohydrates, plant oils, polyesters, polyethers, films

ABSTRACT

One of the challenges of developing bio-derived polymers is to obtain materials with competitive properties. This study investigates the structure-properties relationships of polyesters and polyethers that can be derived from D-xylose through metathesis polymerisation, in order to produce bio-derived plastic materials that are sourced from sustainable feedstocks and whose properties can compete with polyolefins such as polyethylene. Bicyclic diol 1,2-O-isopropylidene-α-D-xylofuranose (IPXF) was coupled with ω-unsaturated fatty acids and alcohols of different chain length ($C_{11}$, $C_5$, $C_3$), and the resulting α,ω-unsaturated esters and ethers polymerized via acyclic diene metathesis (ADMET) polymerization using commercial Grubbs 2$^{nd}$ generation catalyst, obtaining polymers with $M_n$ up to 63.0 kg mol$^{-1}$. Glass transition temperatures ($T_g$) decreased linearly with increasing chain length and were lower for polyethers (–32 to 14 °C) compared to polyesters (–14 to 45 °C). ADMET polymers could be modified post-polymerization by reaction of their internal carbon-carbon double bonds. Thiol-ene reaction lowered $T_g$ while allowing insertion of additional functional groups. Alkene hydrogenation turned the polyester and polyether with $C_{20}$ hydrocarbon linkers into semicrystalline polymers with $T_m$ ~50 °C. The latter, when cast into films, displayed remarkable polyethylene-like properties. Hot-pressed films proved ductile materials (Young modulus $E_y$ 60-110 MPa, elongation at break $\varepsilon_b$ 670–1000%, ultimate tensile strength $\sigma_b$ 8–10 MPa), while uniaxially-oriented films proved very strong yet flexible materials ($E_y$ 190-200 MPa, $\varepsilon_b$ 160–350%, $\sigma_b$ 43–66 MPa). Gas barrier properties were comparable to commercial polyolefins. Polyethers were resistant to hydrolysis while polyesters depolymerized under alkaline conditions.

## Introduction

Driven by environmental persistence and dependence on fossil feedstocks of commercial plastics, research into biobased polymeric materials has been growing steadily over the past decades, yet only a very limited number of materials has emerged commercially. To be considered as suitable replacements for traditional polymers, ideal materials should firstly be inherently more sustainable alternatives from a whole-system perspective, *i.e.* not displacing their impacts elsewhere (hence, for instance, using feedstocks not only renewable but also abundant and non-detrimental to ecosystems and communities; designing degradable but also durable and recyclable materials). Secondly, they must be competitive solutions in terms of both economic cost and material performance. Satisfying all these criteria represents the true challenge the field presently faces, which has strongly limited market penetration of bioplastics – excluding a few high-value, low-volume specialty materials (such as biomedical products) and higher-volume commodity plastics such as PLA and starch blends which have seen consistent investments for at least four decades.

We argue that one of the promising feedstock to satisfy all these requirements are carbohydrates. With regard to the first criterion mentioned above, carbohydrates are the most abundant biomaterial on Earth, which can be derived from non-edible sources and, more importantly, from waste streams (*e.g.* agricultural, forestry, papermaking waste); they are also highly biodegradable and non-toxic. As for the second criterion, carbohydrates – especially from lignocellulosic biomass – are inexpensive and cost-competitive with petrochemical feedstocks; they display wide structural diversity and functionalizability, which can be exploited for the production of materials with disparate yet highly specific properties. D-xylose is used in this study as it can be easily derived from hemicellulose from second and third generation feedstocks. Plant oils are also an extremely important feedstock for polymer production, thanks to their high C/O

ratio together with their structural diversity and reactivity of ester and alkene (and, in some cases, hydroxyl) functional groups.[1] Already used by the chemical industry on a multi-million-ton scale, their sourcing from crop plants is being targeted for replacement with algae oils, avoiding or limiting the need for arable land, freshwater and fertilizers.

Critically, the design of novel renewable (and potentially degradable) polymers from biomass must target certain key properties (thermal stability, glass transition ($T_g$) and melting ($T_m$) temperatures, processability *etc.*) in order to develop suitable materials for intended applications. To this end, investigation of their structure-properties relationships is paramount. Thus, desired properties can be targeted efficiently, and novel bioplastics can be developed for desired applications as equal or superior substitutes for traditional fossil-based materials.

Polyolefins are currently the main polymer class on the market (PE, PP, PS, PVC together account for 65% of the plastic production in Europe).[2] Despite their excellent properties and low cost, lack on in-chain functional groups inhibits their degradability and chemical recycling, a major drawback for the transition to a circular economy. Hence biobased alternatives to polyolefins, together with displaying comparable or improved material properties, should address said problem. A promising alternative, which has seen rising interest in the last decade, are long-chain aliphatic polyesters (here referred to as lcAPES), recently comprehensively reviewed.[1, 3, 4] Indeed, ester linkages introduce breakable points in the aliphatic chains making these polymers depolymerizable, and potentially chemically recyclable as demonstrated recently by Mecking *et al*.[5] Even if some lcAPES have been recently reported as biodegradable,[6] many remain resistant to hydrolysis and enzymatic degradability because of their elevated crystallinity and hydrophobicity.[7] Besides, lcAPES have also been shown to be biocompatible and non-toxic.[7]

While short- and medium-chain aliphatic polyesters display reduced $T_m$ compared to polyolefins, lcAPES – thanks to their extended methylene groups chains – show crystalline behavior similar to HDPE and are therefore often called "polyethylene-like" materials or PE mimics. Other alternatives are long-chain aliphatic polyamides, polycarbonates, polyethers, polythioethers *etc*.[3, 4] Monomers for lcAPES can be derived from unsaturated fatty acids (including from algae oils)[8] *via* a range of catalytic processes, including olefin metathesis (self- and cross-metathesis), isomerization-alkoxycarbonylation, hydroformylation, hydroboration. Polymerization techniques used are chiefly polycondensation of diacids and diols (the latter by reduction of the former) or hydroxyacids, acyclic diene metathesis (ADMET) polymerization of dienes and (tandem or sequential) hydrogenation; and, to a lesser extent, ring opening polymerization (ROP) of macrolactones and ring opening metathesis polymerization (ROMP)/hydrogenation.

A number of recent studies on lcAPES allowed to establish precise structure-properties relationships. Importantly, $T_m$ is known to increase with increasing $CH_2/CO_2$ ratio following a linear trend predicting a $T_m$ of 134 °C for $CH_2/CO_2 \rightarrow \infty$, which equals the experimental $T_m$ for HDPE, and explains the polyethylene-like crystalline nature of lcAPES.[4, 9] Moreover, branching lowers lcAPES $T_g$ and converts them into (L)LDPE mimics.[10] Finally, insertion of a central bulky core (often sugar-derived) in the monomers has been shown to give additional properties depending on its nature (for instance improved mechanical properties and shape memory effects,[11, 12] increased $T_m$).[13]

Recently, we have reported the synthesis of unsaturated lcAPES *via* ADMET containing rigid monosaccharide cores.[14] More specifically, isopropylidene-protected D-xylose (O-isopropylidene-α-D-xylofuranose, IPXF) and D-mannose, and 10-undecenoic acid from castor oil

were combined into α,ω-diene monomers which were then polymerized with Grubbs second generation catalyst, obtaining high molar mass unsaturated lcAPES ($M_n$ up to 71.4 kg mol$^{-1}$). Polymers were highly thermally (up to 330-355 °C) and hydrolytically stable amorphous rubbers ($T_g$ −28 to −8 °C). Post-polymerization ketal deprotection on the sugar cores induced semicrystallinity ($T_m$ 48-49 °C) and allowed casting of transparent polymer films; OH functionalization was also demonstrated. Notwithstanding the versatility added by the sugar cores to these lcAPES, their thermo-mechanical properties were not competitive. Therefore, it was deemed interesting to explore variations of the aliphatic component as well as studying different linkages (*i.e.* ether) and post-polymerization modifications to give fully saturated (including with side chains) APES, in order to establish these polymers as a versatile platform for sustainable functional materials. Herein we report the synthesis and modification of a series of xylose-derived aliphatic polyesters and polyethers, and we reveal their structure-properties relationships. This understanding has ultimately culminated into the development of a renewable polyether with polyethylene-like properties, including mechanical and gas barrier properties comparable to commercial polyolefins.

## Results and discussion

### Synthesis of monomers

As alternatives to the 10-undecenoic acid co-building block used previously,[14] we selected fatty acids of different chain length, namely 4-pentenoic acid ($C_5$) and acrylic acid ($C_3$). Despite being today almost exclusively sourced from petrochemical feedstocks, both acids can be produced from biomass: pentenoic acid from levulinic acid *via* γ-valerolactone,[15-17] while acrylic acid, key intermediate for the polymer industry, from lactic acid *via* dehydration,[18] or from glycerol through

a number of routes.[19] Additionally, we intended to investigate the effect of a different chemical linkage between sugar and hydrocarbon moieties, and replace the ester functionality with its ether counterpart. To this end, instead of carrying a challenging hydrogenation of carbonyl moieties to methylene groups post-polymerization,[20] we opted for the synthesis of ether-containing acyclic diene monomers by a nucleophilic substitution of alcohol derivatives with IPXF. Therefore, we selected the alcohol analogues of the abovementioned acids, namely 10-undecenol ($C_{11}$), 4-pentenol ($C_5$) (both obtainable from biomass *via* the acids) and allyl alcohol ($C_3$, an important industrial intermediate). Substitution of ester with ether groups should provide more flexible polymer chains, together with higher chemical stability essential for certain applications.[20]

**Scheme 1.** Synthesis of ADMET monomers and polymers from IPXF: polyesters (top) and polyethers (bottom). **1a** and **poly(1a)** were reported in our previous work[14] and inserted here for completeness and to account for its post-polymerization modification (see Scheme 2)

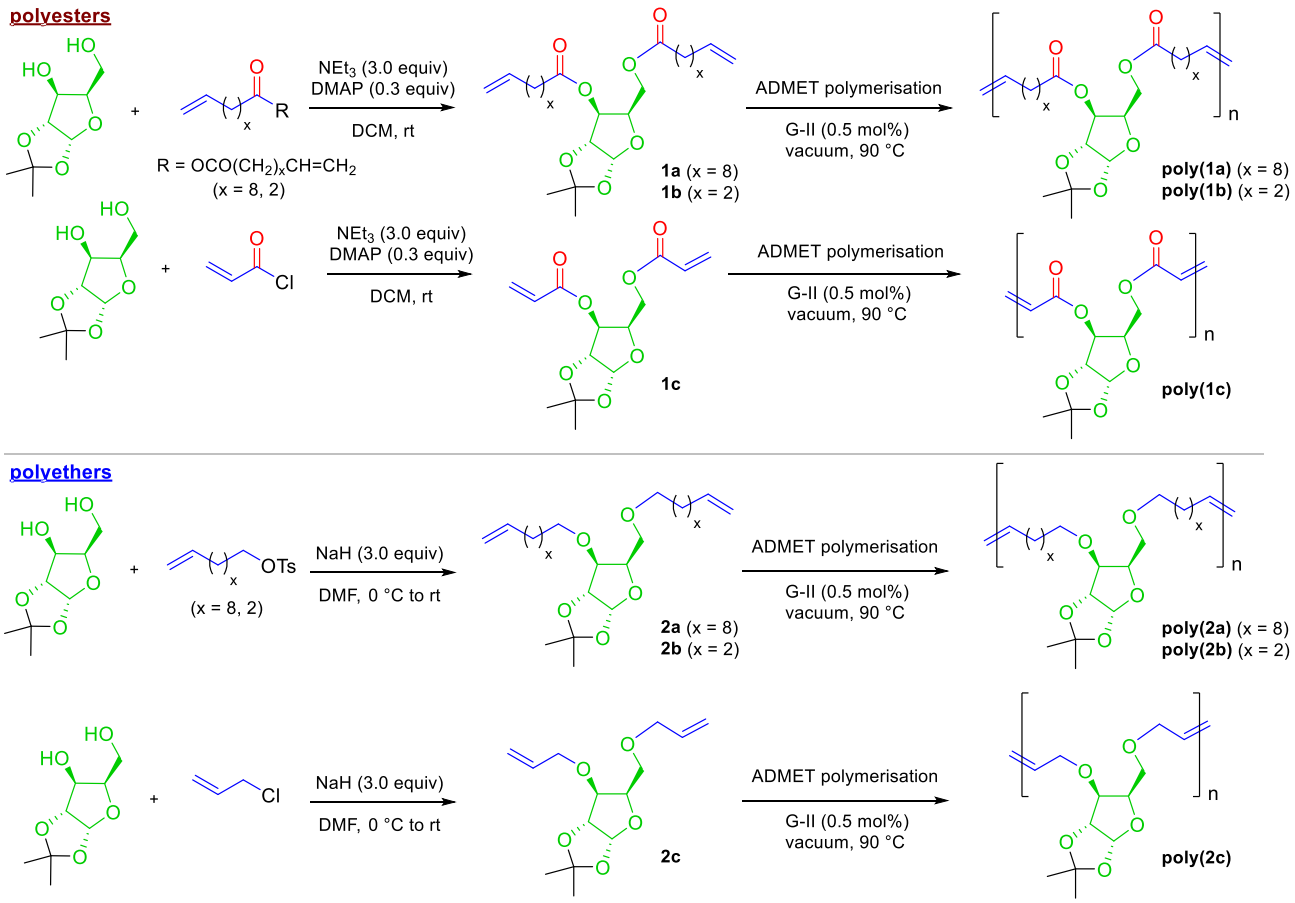


Diene diester **1b** was easily synthesized according to our previous report for **1a**,[14] by esterification of IPXF with 4-pentenoyl anhydride (obtained by transanhydrification of 4-pentenoic acid with acetic anhydride) using triethylamine/4-(dimethylamino)pyridine as catalytic system (Scheme 1, top). For the synthesis of diester **1c**, as acryloyl anhydride could not be isolated due to the formation of polymeric material, commercial acryloyl chloride was used for the esterification under the same conditions. Diene diethers **2a** and **2b** were obtained *via* nucleophilic attack of IPXF on the *p*-toluenesulfonate derivatives of 10-undecenol and 4-pentenol, respectively, using NaH as base in dimethylformamide (Scheme 1, bottom). For the diether **2c**, as allyl *p*-toluenesulfonate could not be isolated with sufficient purity despite several methods attempted, commercial allyl chloride was used as alternative following the same etherification procedure. All

monomers were purified *via* column chromatography prior to polymerization; in addition, **2a** obtained without chromatographic purification was also successfully polymerized (see below).

**ADMET polymerization**

ADMET polymerization of the thus obtained xylose-derived α,ω-diene monomers was performed according to the previously reported procedure, using Grubbs second generation catalyst (G-II).[14] In particular, the best conditions previously found were here employed: 0.5 mol% G-II, 90 °C, bulk, dynamic vacuum (1-20 mbar), mechanical stirring. It is worth remarking that these conditions, especially use of low catalyst loading (which could be further reduced to 0.1 mol%)[14] and no solvent, are advantageous in terms of sustainability and cost. Polymerization was confirmed via $^{1}$H NMR spectroscopy (disappearance of terminal olefin signals at *ca.* 5.0 and 5.8 ppm and appearance of new internal olefin signals at 5.6–5.8 ppm; see Figure 1) and size exclusion chromatography (SEC). As already observed by us and other authors, configuration of the internal alkene is prevalently *trans* and minor olefin position isomerization occurs due to the relatively high temperature used.[14, 21] This was however not investigated further as later development focused on saturated materials (*vide infra*). Polymers were obtained with a number average molar mass ($M_n$) in the range 12.7–63.0 kg mol$^{-1}$, except for **poly(1c)**, which was found insoluble in all common solvents and could not be analyzed (its polymeric and molecular structure is therefore postulated but in agreement in later $T_g$ trends), and **poly(2c)**, which could only be obtained with a $M_n$ of only 1.7 kg mol$^{-1}$ (Table 1). We propose that these molar masses correlate with the monomer structure, in that shorter $M_n$ were obtained for monomers in which alkene groups are closer to the central sugar core. Indeed, it is known that coordinating and/or sterically hindered groups not sufficiently spaced from the polymerizable olefin moieties can inhibit ADMET catalyst activity.[22] However, this effect was not investigated further as falling beyond the scope of the study.

Regardless, it is worth emphasizing that the high molar mass obtained for **poly(2a)** mirrors that observed for the previously reported ester analogue **poly(1a)** (Table 1).[14]

Additionally, as a proof of concept, diene diether **2a** obtained without chromatographic purifications (solely through simple solvent extraction) was polymerized under the same conditions, yielding **poly(2a)** with $M_n$ 12.4 kg mol$^{-1}$ ($Đ_M$ 1.99). While this molar mass is lower than that obtained from a monomer purified by chromatography, it demonstrates the possibility of reducing costs and environmental impact (chiefly, material requirements and waste generation) of the process, without drastically affecting product performance.

**Table 1.** ADMET polymerization of xylose-derived α,ω-diene monomers [a]

| monomer | conv. % (NMR) [b] | yield % | $M_{n,\,SEC}$ [c] kg mol$^{-1}$ | $Đ_{M,\,SEC}$ [c] |
|---|---|---|---|---|
| **1a** [d] | 100 | 70 | 71.4 | 2.15 |
| **1b** | 98 | 74 | 25.0 | 4. 67 |
| **1c** [e] | n.d. [e] | 21 | n.d. [e] | n.d. [e] |
| **2a** | 100 | 96 | 63.0 | 2.12 |
| **2b** [f] | 100 | 77 | 12.7 | 1.55 |
| **2c** [g] | n.d. [g] | 43 [g] | 1.7 [g] | 2.86 [g] |

[a] General conditions: α,ω-diene monomer (1.0 g, 1.0 equiv), G-II (0.005 equiv); 90 °C, bulk, dynamic vacuum (1–20 mbar), 20 hrs. [b] Monomer conversion determined *via* $^1$H NMR spectroscopy by integral ratio of sugar signal at 5.9-6.0 ppm and terminal olefin signal at 5.8 ppm. [c] Molar masses determined on the polymer after precipitation in methanol *via* size exclusion chromatography (SEC) in THF using polystyrene standards calibration. [d] Data from our previous work[14] reported here for comparison. [e] Solid monomer; polymerization performed in propylene carbonate (5 mL) on 0.25 g of monomer at 100 mbar; resulting polymer was insoluble thus preventing NMR and SEC analysis. [f] Polymerization run for 3 hrs, after which 0.005 equiv G-II were added and the polymerization was allowed to continue for 17 hrs; total 20 hrs. [g] Conversion not determined due to overlapping $^1$H NMR signals; yield and molar mass distribution assessed on the crude polymer without precipitation.

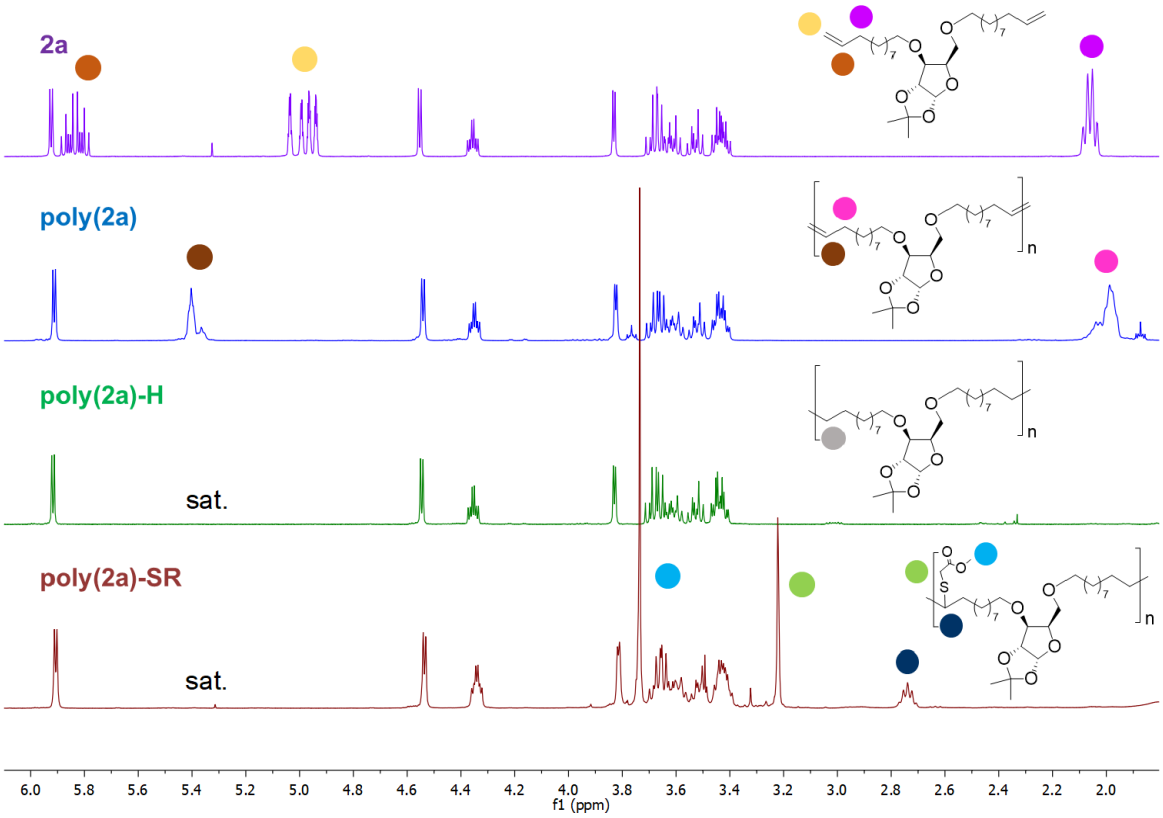


**Figure 1.** Stacked $^{1}$H NMR spectra portion of (from top to bottom) **2a**, **poly(2a)**, **poly(2a)-H** and **poly(2a)-SR**, with distinctive functional groups and corresponding NMR signals marked by colored circles (*sat.* indicates the saturation/disappearance of internal olefin signals).

**Post-polymerization modifications**

ADMET polymers (except the insoluble **poly(1c)** and the oligomeric **poly(2c)**) were chemically modified in post-polymerization reactions, specifically targeting the newly formed internal olefin groups. This approach adds to the previously explored post-polymerization ketal deprotection and OH functionalization,[14] widening the synthetic possibilities of this polymer platform. Firstly, polymers were subjected to C=C reduction to give the saturated counterparts (Scheme 2, right), in order to evaluate the impact of the more flexible saturated hydrocarbon segments on polymer

properties. Following a common procedure using *p*-toluenesulfonyl hydrazide as reducing agent (using hydrogen over Pd/C was also possible albeit with lower conversions),[23] alkene bonds were hydrogenated quantitatively as confirmed by the disappearance of the characteristic signals in the $^1$H NMR spectra (5.4–5.6 ppm, see Figure 1 for a representative example for **poly(2a)**). It is worth emphasizing that reduction of internal olefins in ADMET polymers provides polyethylene-like segments in the resulting polymers, as already well demonstrated for several lcAPES.[1, 3, 4] Here, it accentuates the structural difference between highly rigid IPXF cores and flexible hydrocarbon linkers.

**Scheme 2.** Post-polymerization modification of C=C bonds on ADMET polymers backbone: thiol-ene functionalization (left), olefin reduction (right)

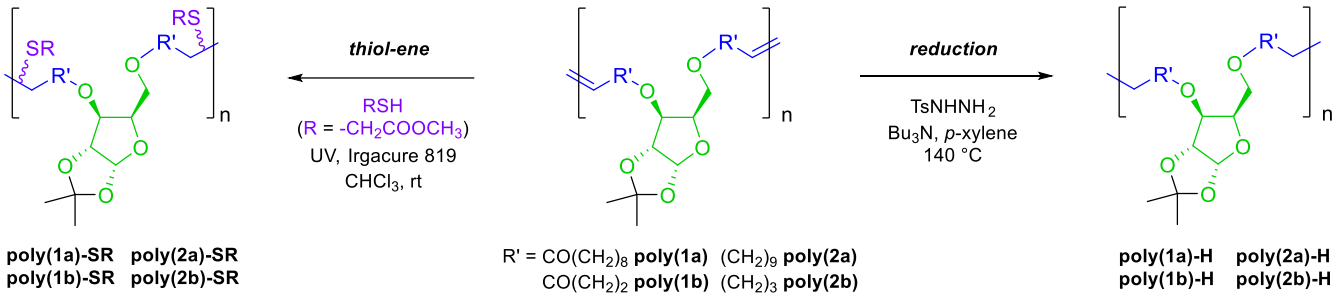


Secondly, the reactivity of the internal olefin in a typical thiol-ene "click" reaction was tested, using methyl thioglycolate as representative thiol (Scheme 2, left). The reaction, performed at room temperature under UV light in presence of Irgacure 819 as photoinitiator, gave complete conversion to the expected product for all polymers, as confirmed by NMR spectroscopy (disappearance of olefin signals in the $^1$H NMR spectra, see example in Figure 1 and Figures S42, S45, S48, S51, and HMBC coupling between thiol methylene protons at 3.2 ppm and asymmetric carbon on polymer backbone at 46–47 ppm, Figures S44, S47, S50, S53), while preserving the

polymeric nature of the materials (albeit a 16 to 59% $M_n$ decrease, see Table S2, which could be reduced by optimizing reaction conditions). This easy functionalization further demonstrates the versatility of this polymer class, suggesting a variety of possible post-polymerization modifications such as introduction of different side chains to tune polymer properties (such as glass transition temperature)[24] or insert functional groups for targeted applications.

**Polymer characterization and structure-properties relationships**

**Thermal properties.** Structure-properties relationships of ADMET polymers and their derivatives were investigated primarily by assessment of their thermal properties, determined *via* differential scanning calorimetry (DSC) and thermogravimetric analysis (TGA) (Table 2). DSC revealed significant variations in glass transition ($T_g$) and melting ($T_m$) temperatures for polymers with different structures (Figure 2). Firstly, as could be expected, decreasing length of hydrocarbon linker chains induced a considerable increase on $T_g$ for both **poly(1)** and **poly(2)** series. Remarkably, this trend was found to be roughly linear against the number of carbon atoms in hydrocarbon linkers for both series (Figure 3). Specifically, for poly(ene esters) $T_g$ increased from –14 °C for the previously reported **poly(1a)** ($C_{20}$ linkers) to 36 °C for **poly(1b)** ($C_8$ spacers), to 45 °C for **poly(1c)** ($C_4$ linkers). Similarly, for poly(ene ethers) $T_g$ increased from –32 °C for **poly(2a)** to 0 °C for **poly(2b)**, to 14 °C for **poly(2c)**. This effect clearly arises from the lower polymer chain flexibility where rigid IPXF cores are connected by shorter flexible hydrocarbon linkers; this induces higher stiffness in the polymer backbone and ultimately lower mobility. The effect of substituting ester with ether functionalities was also remarkable, with polyethers showing significantly lower (18 to 36 °C difference) $T_g$ compared to polyesters. This effect was expected based on the higher flexibility of polyethers caused by the free rotation of $sp^3$ methylene groups in ethers compared to $sp^2$ carbonyl moieties of esters (Figures 2-3).

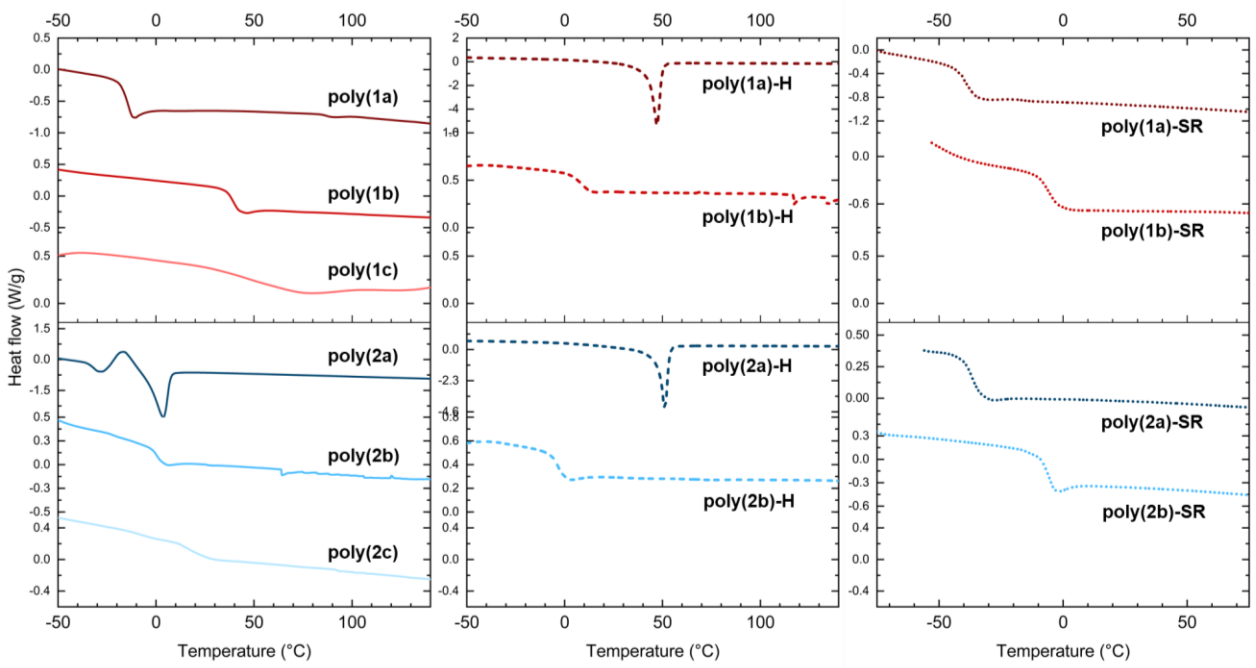


**Figure 2**. DSC traces portion for ADMET polymers (left), saturated polymers (middle) and thiol-ene modified polymers (right) (second DSC heating cycles, except for **poly(1c)** first heating cycle).

**Table 2.** Thermal properties of ADMET polymers and their post-polymerization derivatives as determined *via* DSC (under $N_2$) and TGA (under Ar)

| Polymer | $T_g$ [a] | $T_m$ [b] ($H_m$) [c] | $T_{d5\%}$ [d] | $T_{inf}$ [e] (mass loss) [f] | | residual mass [g] |
|---|---|---|---|---|---|---|
| | °C | °C (J $g^{-1}$) | °C | °C (%) | | % |
| **poly(1a)** [h] | –14 | n.d. | 335 | 340 (60.4) | 442 (23.5) | 15.6 |
| **poly(1b)** | 36 | n.d. | 288 | 325 (84.1) | | 12.9 |
| **poly(1c)** [i] | 45 [j] | n.d. | 309 | 327 (53.0) | 412 (25.2) | 21.5 |
| **poly(2a)** | –32 | 4 (27.4) | 318 | 385 (90.0) | | 8.8 |
| **poly(2b)** | 0 | n.d. | 270 | 355 (85.0) | | 11.0 |
| **poly(2c)** | 14 | n.d. | 129 | 163 (16.0) | 294 (68.7) | 11.7 |

| | | | | | | |
|---|---|---|---|---|---|---|
| **poly(1a)-H** | 33 [j] | 44 (40.5) | 267 | 313 (78.2) | | 7.7 |
| **poly(1b)-H** | 9 | n.d. | 229 | 284 (80.7) | | 17.4 |
| **poly(2a)-H** | 23 [k] | 50 (41.8) | 278 | 343 (64.2) | 393 (23.0) | 6.6 |
| **poly(2b)-H** | –3 | n.d. | 203 | 202 (20.5) | 299 (60.0) | 20.3 |
| **poly(1a)-SR** | –40 | n.d. | 267 | 340 (60.3) | 431 (19.4) | 16.5 |
| **poly(1b)-SR** | –6 | n.d. | 278 | 300 (83.2) | | 16.8 |
| **poly(2a)-SR** | –37 | n.d. | 264 | 382 (89.4) | | 10.6 |
| **poly(2b)-SR** | –5 | n.d. | 277 | 328 (84.6) | | 15.4 |

[a] Glass transition temperature determined for the second heating cycle. [b] Melting temperature determined for the second heating cycle (n.d.: not detected).[c] Enthalpy of fusion determined for the corresponding melting temperature. [d] Temperature at which 5% mass loss is observed. [e] Temperature at which maximum mass loss is observed for the considered decomposition step. [f] Relative mass loss for the considered decomposition step. [g] Residual mass at 600 °C. [h] Data previously reported[14] inserted here for comparison. [i] The polymeric nature of **poly(1c)** could not be demonstrated by conventional methods (NMR spectroscopy, SEC) as insoluble; see Table 1 footnote e. [j] Determined for the first heating cycle. [k] Determined for both first and second cooling cycles.

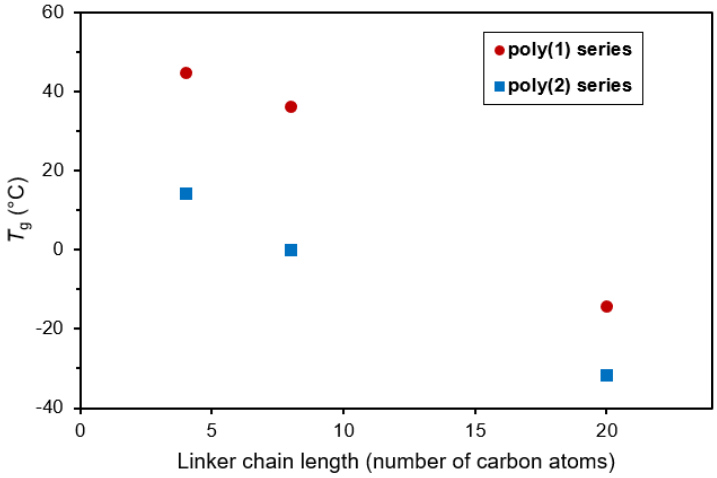


**Figure 3.** Correlation between glass transition temperature ($T_g$) and linker chain length for unsaturated ADMET polymers (**poly(1)** series: polyesters; **poly(2)** series: polyethers).

All unmodified ADMET polymers were found to be amorphous, as evidenced from their lack of $T_m$, except for **poly(2a)** which proved to melt at 4 °C and crystallize at –23 °C. This peculiar behavior was ascribed to the structure of this polymer, consisting in highly-spaced IPXF cores connected *via* ether bonds by long ($C_{20}$) highly flexible (yet unsaturated) hydrocarbon linkers, allowing for the close packing of hydrocarbon segments into crystalline domains.

This hypothesis was further supported by the thermal features of hydrogenated ADMET polymers. While hydrogenated poly(ene esters) and poly(ene ethers) with $C_8$ and $C_4$ linkers were found to be amorphous, **poly(1a)-H** and **poly(2a)-H** (with $C_{20}$ linkers) displayed sharp endothermic peaks at 44 and 50 °C, respectively. Reduction of internal alkenes to alkanes clearly allows crystallization of $C_{18}/C_{20}$ polyethylene-like segments, phenomenon well-known for lcAPES,[1, 3, 4] magnifying in this case the crystalline behavior already observed for the unsaturated polyether **poly(2a)** and converting the amorphous unsaturated polyester **poly(1a)** into a semicrystalline material. Remarkably, the presence of in-chain bicyclic saccharide cores does not prevent crystallization (except for polymers with shorter $C_8$ linkers). However, it significantly reduces $T_m$ compared to values reported for saturated aliphatic $C_{20}$ lcAPES (~100 °C).[9] This effect may represent an advantage to increase the known limited hydrolyzability/degradability of lcAPES. Hydrogenation lowered $T_g$ significantly for **poly(1b)** (from 36 to 9 °C) and marginally for **poly(2b)** (from 0 to –3 °C) (Table 2, Figure S66). No $T_g$ was detected in the second DSC cycle for **poly(1a)-H** and **poly(2a)-H**, possibly because of their elevated crystallinity (and consequently small amorphous domains). Yet, for both polymers, first DSC heating cycles showed very small yet significantly upshifted $T_g$ (33 and 23 °C respectively, representing variations of +47 and +55 °C); however this trend cannot be generalized.

Thiol-ene functionalization of ADMET polymers with methyl thioglycolate led to a decrease of $T_g$ for all four polymers, as could be expected from the addition of aliphatic and relatively flexible side chains to the polymer backbone (Table 2, Figure 2, Figure S66). $T_g$ was found particularly low for polymers with $C_{20}$ linkers (–40 °C for **poly(1a)-SR** and –37 °C for **poly(2a)-SR**), and higher yet still reduced for $C_8$ linkers (–6 °C for **poly(1b)-SR** and –5 °C for **poly(2b)-SR**). Yet, the $T_g$ decrease compared to ADMET precursors appeared prominent for polyesters ($\Delta T_g$ = –26 and –42 °C for **poly(1a)-SR** and **poly(1b)-SR**, respectively), and less pronounced for polyethers ($\Delta T_g$ = –5 °C for both). This evidence once again demonstrates the higher mobility of polyether chains, for which thiol-ene functionalization does not increase the overall polymer free volume. The progressive reduction of $T_g$ with increasing pendant group length is a well-known effect in polymer chemistry and was recently demonstrated for carbohydrate-based polycarbonates.[24] Although a more systematic investigation in this sense falls beyond the scope of this study, we have demonstrated that thiol-ene reactions can be used for sugar-containing ADMET polymers to modify both their physical properties and their functionality.

Thermogravimetric analysis (TGA) carried out under Ar atmosphere showed all ADMET and post-modified polymers to be highly thermally stable (Table 2, Figures S81-S82), with initial 5% mass loss measured in the range of 203–335 °C ($T_{d5\%}$; except for the oligomeric **poly(2c)**). As-synthesized ADMET polymers were found particularly stable, with $T_{d5\%}$ of 270–335 °C and maximum decomposition rate observed at 325–385 °C. Hydrogenated samples showed slightly reduced yet good stability ($T_{d5\%}$ 203–278 °C), possibly due to partially decreased molar masses and/or presence of impurities. Thiol-ene modified polymers showed relatively high decomposition temperatures in a narrow range ($T_{d5\%}$ 264–278 °C). The residual mass present at 600 °C ranged from 6.6 to 21.5%, with however no trends identifiable.


**Figure 4**. Photograph of the film produced from **poly(2a)-H** (diam. 50 mm, thickness 170 μm).

**Mechanical properties.** **Poly(1a)-H** and **poly(2a)-H**, most probably thanks to their semicrystallinity, showed tendency to create self-standing films, which was exploited for casting films *via* hot pressing (see Supporting Information). While **poly(1a)-H** gave self-standing yet somewhat brittle films (Figure S99), remarkably **poly(2a)-H** allowed the manufacture of films ranging from 70 to 700 μm in thickness, all displaying good degrees of flexibility, robustness and optical transparency (Figure 4 and Figures S96-S98). This result is noteworthy, especially considering the brittleness we have observed in polymers incorporating rigid carbohydrate cores.[25-27] Mechanical properties of **poly(2a)-H** were investigated by means of uniaxial tensile testing on 40 x 4.0 mm rectangular specimens (gauge length 20 mm; Table 3, Figure 5, Figure S101). Hot-pressed samples with thickness of *ca.* 100 μm displayed, after a short elastic region (up to *ca*. 5% strain, Young modulus $E_y$ = 61 ± 2 MPa), a remarkably extended plastic deformation. The latter was composed by a neck formation and propagation behavior typical of cold drawing, followed,

after *ca*. 450% $\varepsilon$, by a strain hardening region (Figure 5a and Figure S103). Elongation at break was remarkable, $\varepsilon_b$ = 667 ± 18 %, while ultimate tensile strength was $\sigma_b$ = 7.8 ± 0.3 MPa. Films with thickness of *ca.* 700 μm displayed similar behavior but greater figures, with $\varepsilon_b$ = 1000 ± 40 % and $\sigma_b$ = 9.7 ± 0.5 MPa (Figure S101). Remarkably, after being tested, all specimens were found to be even stronger materials. After breakage, likely occurring at a weak point in the polymeric film, the overall specimen length was reduced to approximately two thirds of the final measured displacement, suggesting a viscoelastic rather than a purely plastic behavior (Figure 5b). This behavior might be due to the dual nature (hard/soft) of saccharide and paraffinic blocks, often exploited for the production of thermoplastic elastomers, including from lcAPES.[28] Moreover, optical properties of films changed during stretching, turning from transparent to translucent, possibly indicating an increase in crystallinity. Indeed, DSC showed a 50% increase in the energy required for melting stretched samples compared to hot-pressed precursors (Figure S67). These observations suggest that **poly(2a)-H** chains align during elongation and produce uniaxially-oriented films. Thus, portions of these films were re-analyzed *via* tensile testing under identical conditions, providing remarkable results (Figure 5a). Thinner films showed a doubled linear elastic region (up to *ca.* 10% strain) with a three-fold increase in elastic modulus ($E_y$ = 186 ± 9 MPa). Following a steep elastic deformation, ultimate tensile strength showed a larger than 5-fold increase ($\sigma_b$ = 43 ± 2 MPa), mirrored by a 4-fold decrease in stress at break ($\varepsilon_b$ = 155 ± 4 %). Similarly, thicker oriented films displayed a 7-fold increase in $\sigma_b$ (66 ± 6 MPa) and a 3-fold reduction in $\varepsilon_b$ (350 ± 30 %) compared to their hot-pressed precursors. Mechanical recycling of **poly(2a)-H** films *via* hot-pressing of used tensile specimens into new films proved effective, with full recovery of mechanical properties.

Compared to hydrogenated polyether **poly(2a)-H,** polyester analogue **poly(1a)-H** films were found to be brittle, with slightly higher elastic modulus (92 ± 3 MPa) and halved tensile strength (3.9 ± 0.2 MPa), and low elongation at break (9 ± 1 %) (Table 3, Figure S102). The different behavior observed for **poly(2a)-H** and **poly(1a)-H** might be attributed once again to the flexibility difference of polyester and polyether and, to a lesser extent, to the molar mass difference (58.5 and 10.6 kg mol$^{-1}$ $M_n$, respectively).

The exceptional mechanical properties obtained for **poly(2a)-H** are comparable to those typically reported for polyolefins such as polyethylene (for HDPE $E_y$ ~900 MPa, $\sigma_b$ 23-27 MPa, $\varepsilon_b$ 400–900 %),[29, 30] correlating well with the polyethylene-like structure given by the linear $(CH_2)_{20}$ chains. Similar tensile properties have also been observed for a number of lcAPES ($E_y$ 290-450 MPa, $\sigma_b$ 14-18 MPa, $\varepsilon_b$ 580-700 % for PES-15, PES-19,19 and PES-23,23;[*, 31, 32] $E_y$ 910 MPa, $\sigma_b$ 21 MPa, $\varepsilon_b$ 470 % for PES-18,18).[5] Moreover, it is interesting to compare these properties with those obtained by Reineke and coworkers for unsaturated ADMET lcAPES synthesized from 10-undecenoic acid and biobased heterocyclic diols (isosorbide, glucarodilactone, bis(hydroxymethyl)furan).[11, 12] All homopolymers were brittle, while only copolymers containing glucarodilactone displayed high mechanical strength and elasticity ($E_y$ 2-18 MPa, $\sigma_b$ 3-29 MPa, $\varepsilon_b$ 480-1400 %). For the polymers described in this study, **poly(1a)-H** is comparable with said brittle homopolymers, while **poly(2a)-H** demonstrates that it is possible to incorporate in-chain heterocycles without having to recur to copolymerization to obtain advantageous material properties. Overall, we conclude that incorporation of rigid saccharide cores does not impair

[*] The nomenclature used here for lcAPES mirrors that traditionally used for polyamides: PES-X indicates an homopolymer obtained from a $C_X$ hydroxyester or lactone, PES-Y,Z a copolymer obtained from a $C_Y$ diester and a $C_Z$ diol.

mechanical properties of lcAPES, and that sugar units may even provide thermoplastic elastomeric behavior, additional functionalizable sites,[14] and potentially enhanced biocompatibility and (bio)degradability.

**Table 3.** Mechanical properties of polymer films as obtained from uniaxial tensile testing

| polymer | film [a] | $E_y$ [b] *MPa* | $\sigma_b$ [c] *MPa* | $\varepsilon_b$ [d] *%* |
|---|---|---|---|---|
| **poly(2a)-H** | 100 µm hot-pressed | 61 ± 2 | 7.8 ± 0.3 | 667 ± 18 |
| **poly(2a)-H** | 100 µm oriented | 186 ± 9 | 43 ± 2 | 155 ± 4 |
| **poly(2a)-H** | 700 µm hot-pressed | 110 ± 20 | 9.7 ± 0.5 | 1000 ± 40 |
| **poly(2a)-H** | 700 µm oriented | 199 ± 7 | 66 ± 6 | 350 ± 30 |
| **poly(1a)-H** | 100 µm hot-pressed | 92 ± 3 | 3.9 ± 0.2 | 9 ± 1 |

[a] Hot-pressed: film as obtained *via* hot-press casting; oriented: film stretched in previous tensile testing experiment being re-tested; thickness approximate. [b] Young modulus, calculated within the linear 0–5% strain range. [c] Stress at break, coinciding with ultimate tensile strength for all samples. [d] Elongation at break

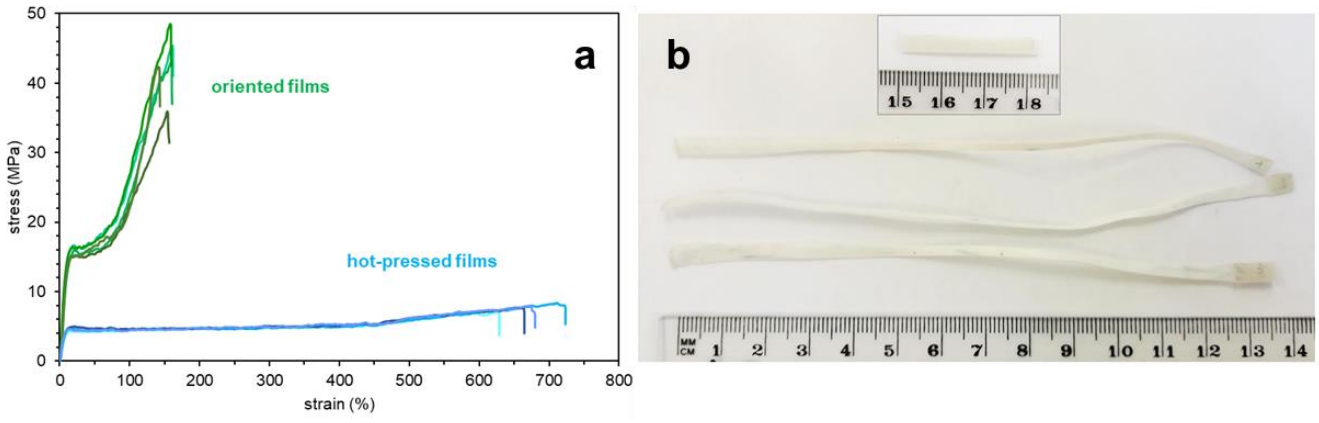


**Figure 5.** (**a**) Stress *versus* strain curves for **poly(2a)-H** films with *ca.* 100 µm thickness, obtained *via* uniaxial tensile testing: comparison of hot-pressed films (blue) and oriented films (stretched in previous tensile test, re-tested; green); (**b**) photographs of **poly(2a)-H** film specimens with *ca.* 700

μm thickness: before (top insert, 30 x 4 mm bar) and after (below) stretching *via* uniaxial tensile testing.

Wide angle X-ray scattering (WAXS) was used to assess polymer film crystallinity and morphological transformations induced by stretching. Hot-pressed **poly(2a)-H** and **poly(1a)-H** samples displayed similar isotropic scattering patterns, with broad peaks likely due to the less efficient polymer chain packing due to the presence of bicyclic IPXF cores, compared to previously reported lcAPES (Figure 6a and Figure S100). Stretched **poly(2a)-H** films, on the other hand, revealed a well-defined anisotropic behavior (Figure 6b-c; see discussion in Supporting Information), typical of axially-oriented polymers, and additional crystallinity, confirming the results obtained from mechanical testing and DSC.

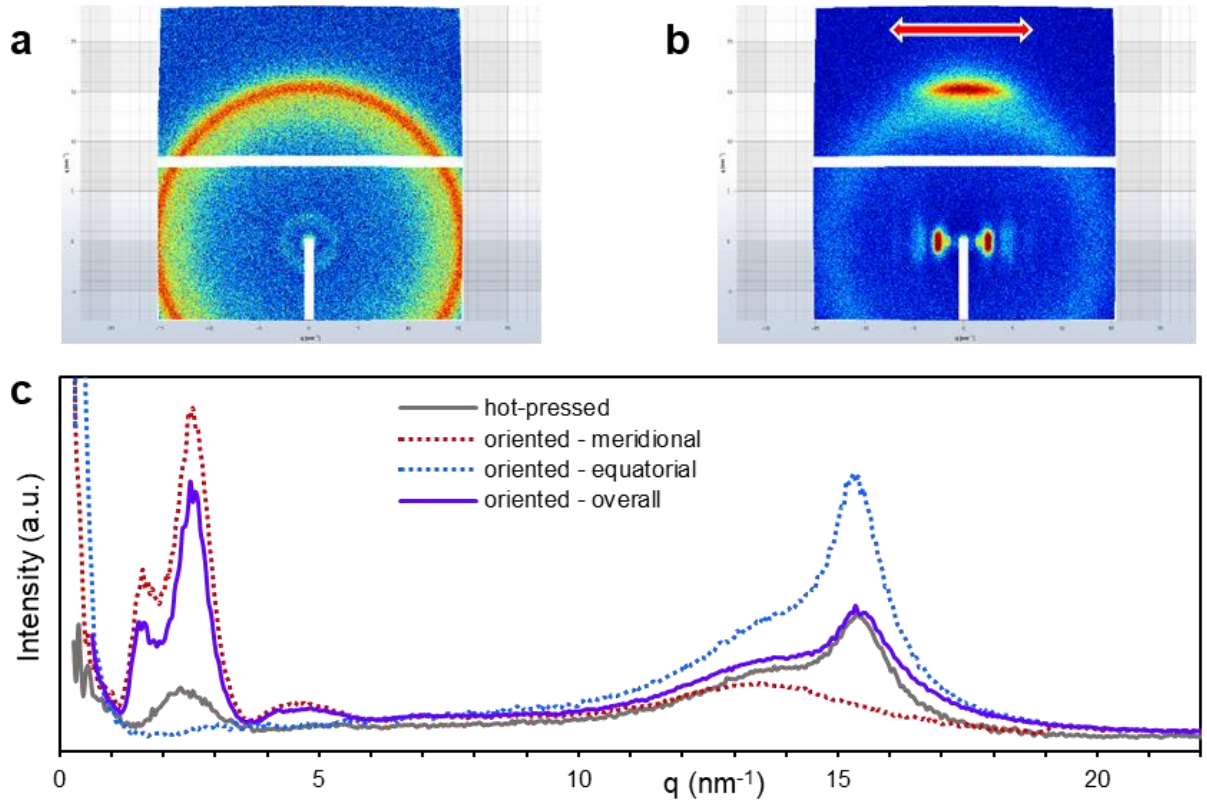

**Figure 6.** WAXS scattering patterns of (**a**) hot-pressed and (**b**) uniaxially-oriented **poly(2a)-H** films (red arrow indicates stretching direction); (**c**) WAXS intensity traces extracted from the above 2D scattering patterns, distinguishing equatorial and meridional contributions

**Barrier properties**. Water contact angle (WCA) for **poly(2a)-H** hot-pressed films was measured as 91 ± 4 °, indicative of a moderately hydrophobic surface. Indeed, this result is similar to literature WCA values for HDPE of ~97 °,[33, 34] and PES-18,18 of 95 °.[5] In contrast, WCA for **poly(1a)-H** films was 78 ± 6 °, suggesting a slightly more hydrophilic polymer, consistent with the presence of polar ester functionalities in place of ether groups.

Gas permeability properties of polymers are important in assessing a material's suitability in packaging applications, wherein high barrier properties are desired. $N_2$, $O_2$, and $CO_2$ permeability values of **poly(2a)-H** were assessed using a differential pressure method, and measured as 0.95 ± 0.09 barrer, 2.00 ± 0.05 barrer and 9.03 ± 0.25 barrer respectively. Interestingly, whist the permeability values of $N_2$ and $O_2$ were constant throughout the measurements, $CO_2$ permeability exhibited an increased dependence over time. This behavior has been widely reported for $CO_2$ permeability in glassy polymers and is associated with swelling of the polymer matrix due to a high penetrant solubility.[35, 36] The gas permeability values measured for **poly(2a)-H**, against which barrier properties are inversely proportional, are competitive with those of many conventional petrochemical plastics, in particular polyolefins (Tables S1 and S3).[37, 38] Specifically, **poly(2a)-H** permeability to $N_2$, $O_2$ and $CO_2$ was found in the same range as LDPE, PP and PS and indeed very close to LLDPE. Compared to literature values for HDPE, **poly(2a)-H** permeabilities were two to three times higher, possibly originated by the reduced chain packing and crystallinity due to the bulky IPXF cores; indeed, gas permeability in polymers has been linked to fractional free volume[39] and structural properties such as chain rigidity,[40, 41] which affect chain

dynamics. The barrier properties of **poly(2a)-H** are also comparable to those reported for lcAPES. Whilst its oxygen permeability falls within the reported range for copolymers of PES-18,6 and its ether-containing analogue (with hexanediol substituted by triethylene glycol), between 1.4 and 2.2 barrer,[42] permeability towards carbon dioxide is halved. In the latter polymer, ether linkages are thought to be responsible for increasing chain flexibility and decreasing crystallinity, leading to higher gas permeation.[42, 43] The presence of an oxygenated heterocycle moiety in **poly(2a)-H**, disrupting chain packing, is most likely to have the same effect here and cause **poly(2a)-H** to have slightly increased permeability values relative to lcAPES PES-X,5 (X = 10-16) reported by Li *et al.* (0.6 – 1.0 barrer).[44] Despite having slightly higher permeability values than other bioderived polymers, including outside the lcAPES category,[45-47] there might be potential to further increase barrier properties of this polymer through processing, by orientating polymer chains to reduce free volume and enhance crystallinity. An alternative approach could implicate removal of isopropylidene groups on xylose cores, so as to induce intermolecular hydrogen bonding and increase crystallinity.[14, 48]

**Polymer degradability**. Finally, polymer degradability under hydrolytic conditions was studied, in order to assess both material stability during use, and possible end-of-life options. In our previous study, unsaturated polyester **poly(1a)** was found stable in the solid state when in contact with aqueous solutions at pH 7, 0 and 14 for as long as 60 days at room temperature.[14] In this study, hydrolytic stability of **poly(2a)-H** and **poly(1a)-H** was assessed by dissolving the semicrystalline polymers in dichloromethane (10 g $L^{-1}$) and adding equal volumes of aqueous HCl or NaOH (1.0 mol $L^{-1}$), then stirring the resulting biphasic mixture at 1500 rpm for 24 hours or 7 days. After removal of the solvents, SEC analysis was used to assess any molar mass variations produced by hydrolysis (Table S4). Polyether **poly(2a)-H** fully retained its molar mass in both

acidic and alkaline conditions. On the other hand, polyester **poly(1a)-H** was found stable to acid-catalyzed hydrolysis, but underwent depolymerization under alkaline conditions. These results, consistent with esters and ethers reactivity, are highly promising for potential applications. As such, polyester **poly(1a)-H** might be used for materials where a certain degradability is desirable, while polyether **poly(2a)-H** might be employed in applications requiring higher chemical stability.[20] Polymers displaying both degradability and elevated mechanical strength could possibly be obtained from saturated random copolymers of **1a** and **2a**. In the wider sustainability context, as demonstrated recently by Mecking and coworkers for lcAPES,[5] **poly(1a)-H** hydrolysis or alcoholysis should allow recovery of IPXF and 1,20-icosanedioic acid, both potentially chemically recyclable – the former into polymers of the same class, the latter for instance into a variety of polycondensation polymers. Moreover, unsaturated ADMET polymers may be depolymerized with ethylene (potentially recovered from ADMET polymerization or biosourced) and possibly chemically recycled.[49] Although biodegradation by enzymes or in real-life conditions falls beyond the scope of this study, we envision its feasibility based on the recently reported biodegradation of unsaturated and saturated long-chain ($C_{18}$) aliphatic polyesters using urban sludge in oxic systems.[6] In comparison, polyesters **poly(1a)** and **poly(1a)-H**, with similar unsaturated and saturated $C_{20}$ chains, also possess monosaccharides cores, which may enhance biodegradability thanks to their intrinsic degradability and to the reduction of polymer crystallinity they induce. Polyethers described in this study may be degradable yet to a lesser extent as relying mainly on sugar decomposition.

## Conclusions

A series of unsaturated polyesters and polyethers were synthesized by ADMET polymerization containing biobased rigid O-isopropylidene-α-D-xylofuranose cores and fatty acids/alcohols

(derived or derivable from biomass) of variable chain length. Molar masses were in the range of 63.0 – 1.7 kg $mol^{-1}$ $M_n$, with a direct correlation with the aliphatic chain length. Post-polymerization modification was conducted on internal alkene bonds *via* hydrogenation and thiol-ene reaction with methyl thioglycolate. Structure-properties relationships were established by means of differential scanning calorimetry and other techniques. Glass transition temperatures for unsaturated ADMET polymers were found decreasing linearly with increasing aliphatic linker chain length, and lower for polyethers (–32 to 14 °C) than for polyesters (–14 to 45 °C) thanks to the higher flexibility given by ether free rotation. While most unsaturated polymers were amorphous, hydrogenation converted $(CH_2)_{18}$/$(CH_2)_{20}$-bearing polyester and polyether into semicrystalline materials, as expected from similar polyethylene-like long-chain aliphatic polyesters (lcAPES). Their melting temperature (44 and 50 °C, respectively) was lower than for lcAPES with comparable $CH_2/CO_2$ ratio (~100 °C), attributed to the presence of bicyclic monosaccharide cores. Nonetheless, polyether **poly(2a)-H** was found highly thermally and hydrolytically stable, with remarkable polyethylene-like properties. Hot-pressed films of a range of thicknesses displayed optical transparency and flexibility. Their tensile properties ($E_y$ 60-110 MPa, $\varepsilon_b$ 670–1000%, $\sigma_b$ 8–10 MPa) and surface energy (water contact angle 91 °) were found comparable to HDPE and similar biobased lcAPES, and superior to other lcAPES homopolymers containing sugar-derived heterocycles. Gas barrier properties were also comparable to commercial polyolefins (and indeed very similar to LLDPE) and other biobased polymers. Moreover, uniaxial film orientation improved crystallinity and tensile properties even further ($E_y$ 190-200 MPa, $\varepsilon_b$ 160–350%, $\sigma_b$ 43–66 MPa), making **poly(2a)-H** a promising candidate for high performance biobased film applications.

Overall, we herein reported a highly versatile class of biobased polymers derived from D-xylose and fatty acids/alcohols, with tunable structure and properties, and several post-polymerization modification strategies, useful for a range of potential applications. Furthermore, we have developed a polyether with remarkable polyolefin-like mechanical and gas barrier properties, representing a promising bioplastic for sustainable packaging applications.

## ASSOCIATED CONTENT

**Supporting Information**. Materials and methods, experimental procedures, characterization data for all compounds, NMR and MS spectra, SEC, DSC and TGA traces for all polymers, SEC data for post-modified polymers, representative photographs of polymer films, additional WAXS data and discussion, additional uniaxial tensile testing data, gas permeability comparative table, hydrolytic stability assessment data (PDF).

## AUTHOR INFORMATION


### Corresponding Author

* a.buchard@bath.ac.uk


### Author Contributions

The manuscript was written through contributions of all authors. All authors have given approval to the final version of the manuscript.


### Funding Sources

The Royal Society (RG/150538, UF/160021 fellowship to AB). The UK EPSRC (EP/L016354/1, studentships to MP and JL, CDT in Sustainable Chemical Technologies).

**Notes**

The authors declare no competing financial interests.

ACKNOWLEDGMENT

The authors acknowledge the Material and Chemical Characterisation Facility (MC²) at the University of Bath (https://doi.org/10.15125/mx6j-3r54) for providing analytical instrumentation, technical support and assistance. We also thank Mrs Clare Ball for the support with tensile testing carried out at the Department of Mechanical Engineering, University of Bath. This work was supported by the Engineering and Physical Sciences Research Council EP/L016354/1 (Studentships to MP and JCL, CDT in Sustainable Chemical Technologies). AB acknowledges Roger and Sue Whorrod (Whorrod Research Fellowship) and the Royal Society (RG/150538; UF/160021 fellowship) for research funding.

ABBREVIATIONS

IPXF: 1,2-O-isopropylidene-α-D-xylofuranose; ADMET: acyclic diene metathesis (polymerization); G-II: Grubbs second generation catalyst; NMR: nuclear magnetic resonance (spectroscopy), SEC: size exclusion chromatography; DSC: differential scanning calorimetry; TGA: thermogravimetric analysis; WAXS: wide-angle X-ray scattering; $T_g$: glass transition temperature; $T_m$: melting temperature; PE: polyethylene; HDPE: high density polyethylene; LDPE: low density polyethylene; LLDPE: linear low density polyethylene; PP: polypropylene; PS: polystyrene; PVC: poly(vinyl chloride); PLA: poly(lactide) or poly(lactic acid); lcAPES: long chain aliphatic polyesters.

REFERENCES

1. Nomura, K.; Binti Awang, N. W. Synthesis of Bio-Based Aliphatic Polyesters from Plant Oils by Efficient Molecular Catalysis: A Selected Survey from Recent Reports. *ACS Sustainable Chem. Eng.* **2021,** *9*, 5486-5505.

2. *Plastics - The Facts 2020*; PlasticsEurope: Brussels, 2021.

3. Maisonneuve, L.; Lebarbé, T.; Grau, E.; Cramail, H. Structure-Properties Relationship of Fatty Acid-Based Thermoplastics as Synthetic Polymer Mimics. *Polym. Chem.* **2013,** *4*, 5472-5517.

4. Stempfle, F.; Ortmann, P.; Mecking, S. Long-Chain Aliphatic Polymers To Bridge the Gap between Semicrystalline Polyolefins and Traditional Polycondensates. *Chem. Rev.* **2016,** *116*, 4597-4641.

5. Häußler, M.; Eck, M.; Rothauer, D.; Mecking, S. Closed-Loop Recycling of Polyethylene-Like Materials. *Nature* **2021,** *590*, 423-427.

6. Roumanet, P.-J.; Jarroux, N.; Goujard, L.; Le Petit, J.; Raoul, Y.; Bennevault, V.; Guégan, P. Synthesis of Linear Polyesters from Monomers Based on 1,18-(Z)-Octadec-9-enedioic Acid and Their Biodegradability. *ACS Sustainable Chem. Eng.* **2020,** *8*, 16853-16860.

7. van der Meulen, I.; de Geus, M.; Antheunis, H.; Deumens, R.; Joosten, E. A. J.; Koning, C. E.; Heise, A. Polymers from Functional Macrolactones as Potential Biomaterials: Enzymatic Ring Opening Polymerization, Biodegradation, and Biocompatibility. *Biomacromolecules* **2008,** *9*, 3404-3410.

8. Roesle, P.; Stempfle, F.; Hess, S. K.; Zimmerer, J.; Río Bártulos, C.; Lepetit, B.; Eckert, A.; Kroth, P. G.; Mecking, S. Synthetic Polyester from Algae Oil. *Angew. Chem., Int. Ed.* **2014,** *53*, 6800-6804.

9. Ortmann, P.; Mecking, S. Long-Spaced Aliphatic Polyesters. *Macromolecules* **2013,** *46*, 7213-7218.

10. Lebarbé, T.; Neqal, M.; Grau, E.; Alfos, C.; Cramail, H. Branched Polyethylene Mimicry by Metathesis Copolymerization of Fatty Acid-Based α,ω-Dienes. *Green Chem.* **2014,** *16*, 1755-1758.

11. Shearouse, W. C.; Lillie, L. M.; Reineke, T. M.; Tolman, W. B. Sustainable Polyesters Derived from Glucose and Castor Oil: Building Block Structure Impacts Properties. *ACS Macro Lett.* **2015,** *4*, 284-288.

12. Lillie, L. M.; Tolman, W. B.; Reineke, T. M. Structure/Property Relationships in Copolymers Comprising Renewable Isosorbide, Glucarodilactone, and 2,5-Bis(hydroxymethyl)furan Subunits. *Polym. Chem.* **2017,** *8*, 3746-3754.

13. Hibert, G.; Grau, E.; Pintori, D.; Lecommandoux, S.; Cramail, H. ADMET Polymerization of α,ω-Unsaturated Glycolipids: Synthesis and Physico-Chemical Properties of the Resulting Polymers. *Polym. Chem.* **2017,** *8*, 3731-3739.

14. Piccini, M.; Leak, D. J.; Chuck, C. J.; Buchard, A. Polymers from Sugars and Unsaturated Fatty Acids: ADMET Polymerisation of Monomers Derived from D-Xylose, D-Mannose and Castor Oil. *Polym. Chem.* **2020,** *11*, 2681-2691.

15. Kumru, B.; Mendoza Mesa, J.; Antonietti, M.; Al-Naji, M. Metal-Free Visible-Light-Induced Dithiol–Ene Clicking via Carbon Nitride to Valorize 4-Pentenoic Acid as a Functional Monomer. *ACS Sustainable Chem. Eng.* **2019,** *7*, 17574-17579.

16. Nobbs, J. D.; Zainal, N. Z. B.; Tan, J.; Drent, E.; Stubbs, L. P.; Li , C.; Lim, S. C. Y.; Kumbang, D. G. A.; van Meurs, M. Bio–based Pentenoic Acids as Intermediates to Higher Value-Added Mono- and Dicarboxylic Acids. *ChemistrySelect* **2016,** *1*, 539-544.

17. Palkovits, R. Pentenoic Acid Pathways for Cellulosic Biofuels. *Angew. Chem., Int. Ed.* **2010,** *49*, 4336-4338.

18. Bonnotte, T.; Paul, S.; Araque, M.; Wojcieszak, R.; Dumeignil, F.; Katryniok, B. Dehydration of Lactic Acid: The State of The Art. *ChemBioEng Rev.* **2018,** *5*, 34-56.

19. Jin, X.; Meng, K.; Zhang, G.; Liu, M.; Song, Y.; Song, Z.; Yang, C. Interfacial Catalysts for Sustainable Chemistry: Advances on Atom and Energy Efficient Glycerol Conversion to Acrylic Acid. *Green Chem.* **2021,** *23*, 51-76.

20. Dannecker, P.-K.; Biermann, U.; Sink, A.; Bloesser, F. R.; Metzger, J. O.; Meier, M. A. R. Fatty Acid–Derived Aliphatic Long Chain Polyethers by a Combination of Catalytic Ester Reduction and ADMET or Thiol-Ene Polymerization. *Macromol. Chem. Phys.* **2019,** *220*, 1800440.

21. Fokou, P. A.; Meier, M. A. R. Use of a Renewable and Degradable Monomer to Study the Temperature-Dependent Olefin Isomerization during ADMET Polymerizations. *J. Am. Chem. Soc.* **2009,** *131*, 1664-65.

22. Caire da Silva, L.; Rojas, G.; Schulz, M. D.; Wagener, K. B. Acyclic Diene Metathesis Polymerization: History, Methods and Applications. *Prog. Polym. Sci.* **2017,** *69*, 79-107.

23. Hillmyer, M. A.; Laredo, W. R.; Grubbs, R. H. Ring-Opening Metathesis Polymerization of Functionalized Cyclooctenes by a Ruthenium-Based Metathesis Catalyst. *Macromolecules* **1995,** *28*, 6311-6316.

24. Song, Y.; Ji, X.; Dong, M.; Li, R.; Lin, Y.-N.; Wang, H.; Wooley, K. L. Advancing the Development of Highly-Functionalizable Glucose-Based Polycarbonates by Tuning of the Glass Transition Temperature. *J. Am. Chem. Soc.* **2018,** *140*, 16053-16057.

25. Gregory, G. L.; Jenisch, L. M.; Charles, B.; Kociok-Köhn, G.; Buchard, A. Polymers from Sugars and $CO_2$: Synthesis and Polymerization of a D-Mannose-Based Cyclic Carbonate. *Macromolecules* **2016,** *49*, 7165-7169.

26. Gregory, G. L.; Kociok-Köhn, G.; Buchard, A. Polymers from Sugars and $CO_2$: Ring-Opening Polymerisation and Copolymerisation of Cyclic Carbonates Derived from 2-Deoxy-D-Ribose. *Polym. Chem.* **2017,** *8*, 2093-2104.

27. Gregory, G. L.; Hierons, E. M.; Kociok-Köhn, G.; Sharma, R. I.; Buchard, A. $CO_2$-Driven Stereochemical Inversion of Sugars to Create Thymidine-Based Polycarbonates by Ring-Opening Polymerisation. *Polym. Chem.* **2017,** *8*, 1714-1721.

28. Stempfle, F.; Schemmer, B.; Oechsle, A.-L.; Mecking, S. Thermoplastic Polyester Elastomers Based on Long-Chain Crystallizable Aliphatic Hard Segments. *Polym. Chem.* **2015,** *6*, 7133-7137.

29. Schmitz, P.; Janocha, S. Films. In *Ullmann's Encyclopedia of Industrial Chemistry*, Wiley-VCH: 2000.

30. Jeremic, D. Polyethylene. In *Ullmann's Encyclopedia of Industrial Chemistry*, Wiley-VCH: 2014; pp 1-42.

31. Stempfle, F.; Ritter, B. S.; Mülhaupt, R.; Mecking, S. Long-Chain Aliphatic Polyesters from Plant Oils for Injection Molding, Film Extrusion and Electrospinning. *Green Chem.* **2014,** *16*, 2008-2014.

32. Cai, J.; Liu, C.; Cai, M.; Zhu, J.; Zuo, F.; Hsiao, B. S.; Gross, R. A. Effects of Molecular Weight on Poly(ω-Pentadecalactone) Mechanical and Thermal Properties. *Polymer* **2010,** *51*, 1088-1099.

33. Salzano de Luna, M.; Galizia, M.; Wojnarowicz, J.; Rosa, R.; Lojkowski, W.; Leonelli, C.; Acierno, D.; Filippone, G. Dispersing Hydrophilic Nanoparticles in Hydrophobic Polymers: HDPE/ZnO Nanocomposites by a Novel Template-Based Approach. *eXPRESS Polym. Lett.* **2014,** *8*, 362.

34. Meemusaw, M.; Magaraphan, R. Surface and Bulk Properties Improvement of HDPE by a Batch Plasma Treatment. *J. Appl. Polym. Sci.* **2016,** *133*, 43011.

35. Barnett, J. W.; Bilchak, C. R.; Wang, Y.; Benicewicz, B. C.; Murdock, L. A.; Bereau, T.; Kumar, S. K. Designing Exceptional Gas-Separation Polymer Membranes Using Machine Learning. *Sci. Adv.* **2020,** *6*, eaaz4301.

36. Minelli, M.; Sarti, G. C. Permeability and Diffusivity of $CO_2$ in Glassy Polymers with and without Plasticization. *J. Membr. Sci.* **2013,** *435*, 176-185.

37. Guisheng, F.; Incarnato, L.; Di Maio, L.; Acierno, D. Discussion About the Use of Relative Values of Permeabilities between Two Gases for High Molecular Weight Polymers. *Polymer* **1995,** *36*, 4345-4346.

38. Siracusa, V. Food Packaging Permeability Behaviour: A Report. *Int. J. Polym. Sci.* **2012,** *2012*, 302029.

39. Sharma, J.; Tewari, K.; Arya, R. K. Diffusion in Polymeric Systems–A Review on Free Volume Theory. *Prog. Org. Coat.* **2017,** *111*, 83-92.

40. Jacobson, S. H. Molecular Modeling Studies of Polymeric Gas Separation and Barrier Materials: Structure and Transport Mechanisms. *Polym. Adv. Technol.* **1994,** *5*, 724-732.

41. Burgess, S. K.; Karvan, O.; Johnson, J. R.; Kriegel, R. M.; Koros, W. J. Oxygen Sorption and Transport in Amorphous Poly(Ethylene Furanoate). *Polymer* **2014,** *55*, 4748-4756.

42. Genovese, L.; Gigli, M.; Lotti, N.; Gazzano, M.; Siracusa, V.; Munari, A.; Dalla Rosa, M. Biodegradable Long Chain Aliphatic Polyesters Containing Ether-Linkages: Synthesis, Solid-State, and Barrier Properties. *Ind. Eng. Chem. Res.* **2014,** *53*, 10965-10973.

43. Gigli, M.; Genovese, L.; Lotti, N.; Munari, A.; Dalla Rosa, M.; Siracusa, V. Gas Barrier and Thermal Behavior of Long Chain Aliphatic Polyesters after Stressed Treatments. *Polym.-Plast. Technol. Eng.* **2017,** *56*, 71-82.

44. Zhou, L.; Wu, L.; Qin, P.; Li, B.-G. Synthesis and Properties of Long Chain Polyesters from Biobased 1,5-Pentanediol and Aliphatic α,ω-Diacids with 10-16 Carbon Atoms. *Polym. Degrad. Stab.* **2021,** *187*, 109546.

45. Komatsuka, T.; Kusakabe, A.; Nagai, K. Characterization and Gas Transport Properties of Poly(Lactic Acid) Blend Membranes. *Desalination* **2008,** *234*, 212-220.

46. Altay, E.; Jang, Y.-J.; Kua, X. Q.; Hillmyer, M. A. Synthesis, Microstructure, and Properties of High-Molar-Mass Polyglycolide Copolymers with Isolated Methyl Defects. *Biomacromolecules* **2021,** *22*, 2532-2543.

47. Zhang, H.; Jiang, M.; Wu, Y.; Li, L.; Wang, Z.; Wang, R.; Zhou, G. Development of High-Molecular-Weight Fully Renewable Biopolyesters Based on Oxabicyclic Diacid and 2,5-Furandicarboxylic Acid: Promising as Packaging and Medical Materials. *ACS Sustainable Chem. Eng.* **2021,** *9*, 6799-6809.

48. White, J. E.; Earls, J. D.; Sherman, J. W.; López, L. C.; Dettloff, M. L. Step-Growth Polymerization of 10,11-Epoxyundecanoic Acid. Synthesis and Properties of a New Hydroxy-Functionalized Thermoplastic Polyester. *Polymer* **2007,** *48*, 3990-3998.

49. Nomura, K.; Chaijaroen, P.; Abdellatif, M. M. Synthesis of Biobased Long-Chain Polyesters by Acyclic Diene Metathesis Polymerization and Tandem Hydrogenation and Depolymerization with Ethylene. *ACS Omega* **2020,** *5*, 18301-18312.

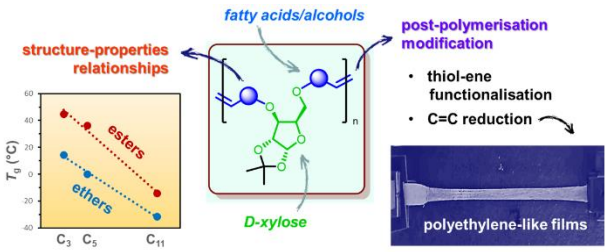


For TOC/Graphical abstract use only